NAVAL POSTGRADUATE SCHOOL
Monterey, California

THESIS

EVALUATION OF A LIQUID-FUELED PULSE DETONATION ENGINE COMBUSTOR

by

David L. Forster

December 1998

Thesis Advisor: David W. Netzer
Co-Advisor: Christopher M. Brophy

Approved for public release; distribution is unlimited.

REPORT DOCUMENTATION PAGE

Form Approved OMB No. 0704-0188

1. AGENCY USE ONLY *(Leave blank)*	2. REPORT DATE	3. REPORT TYPE AND DATES COVERED
	December 1998	Master's Thesis

4. TITLE AND SUBTITLE
EVALUATION OF A LIQUID-FUELED PULSE DETONATION ENGINE COMBUSTOR

5. FUNDING NUMBERS
Contract Number
N0001498WR20018

6. AUTHOR(S)
Forster, David L.

7. PERFORMING ORGANIZATION NAME(S) AND ADDRESS(ES)
Naval Postgraduate School
Monterey, CA 93943-5000

8. PERFORMING ORGANIZATION REPORT NUMBER

SPONSORING / MONITORING AGENCY NAME(S) AND ADDRESS(ES)
Office of Naval Research
Ballston Tower One
800 N. Quincy Street
Arlington, VA 22217-5660

10. SPONSORING / MONITORING AGENCY REPORT NUMBER

11. SUPPLEMENTARY NOTES
The views expressed in this thesis are those of the author and do not reflect the official policy or position of the Department of Defense or the U.S. Government.

12a. DISTRIBUTION / AVAILABILITY STATEMENT
Approved for public release; distribution is unlimited.

12b. DISTRIBUTION CODE

13. ABSTRACT *(maximum 200 words)*

An evaluation of five liquid-fueled pulse detonation engine combustor geometries and flow field conditions was performed over a wide range of equivalence ratios. Particle sizing and spray characterization of commercially available atomizers was conducted to determine the optimum conditions that produced acceptable mass flow and particle size distribution for use in the combustor.

The chosen atomizer was installed in the combustor geometries and then analyzed over a range of combustor conditions to measure deflagration to detonation transition (DDT) distances and detonation wave velocities for each condition. Testing was conducted for ambient (100-110 °F) and higher wall temperatures (>300 °F) at an operating frequency of 5Hz.

It was found that the shortest DDT for JP10 and O_2 was achieved using a stepped front-end insert under hot conditions and with a loaded equivalence ratio greater than .75, but less than 1.15.

14. SUBJECT TERMS
Pulse Detonation Engine, JP10, Liquid Fuels

15. NUMBER OF PAGES
73

16. PRICE CODE

17. SECURITY CLASSIFICATION OF REPORT	18. SECURITY CLASSIFICATION OF THIS PAGE	19. SECURITY CLASSIFI- CATION OF ABSTRACT	20. LIMITATION OF ABSTRACT
Unclassified	Unclassified	Unclassified	UL

NSN 7540-01-280-5500
Prescribed by ANSI std. 239-18

Standard Form 298 (Rev. 2-89)

Approved for public release; distribution is unlimited

EVALUTAION OF A LIQUID –FUELED PULSE DETONATION ENGINE COMBUSTOR

David L. Forster
Lieutenant, United States Navy
B.S., Memphis State University, 1989

Submitted in partial fulfillment of the
Requirements for the degree of

MASTER OF SCIENCE IN ASTRONAUTICAL ENGINEERING

from the

NAVAL POSTGRADUATE SCHOOL
December 1998

Author: _____
David L. Forster

Approved by: _____
David W. Netzer, Thesis Advisor

_____
Christopher M. Brophy, Co-Advisor

_____
Gerald H. Lindsey, Chairman
Department of Aeronautics and Astronautics

ABSTRACT

An evaluation of five liquid-fueled pulse detonation engine combustor geometries and flow field conditions was performed over a wide range of equivalence ratios. Particle sizing and spray characterization of commercially available atomizers was conducted to determine the optimum conditions that produced acceptable mass flow and particle size distribution for use in the combustor.

The chosen atomizer was installed in the combustor geometries and then analyzed over a range of combustor conditions to measure deflagration to detonation transition (DDT) distances and detonation wave velocities for each condition. Testing was conducted for ambient (100-110 °F) and higher wall temperatures (>300 °F) at an operating frequency of 5Hz.

It was found that the shortest DDT for JP10 and O_2 was achieved using a stepped front-end insert under hot conditions and with a loaded equivalence ratio greater than .75, but less than 1.15.

TABLE OF CONTENTS

LIST OF FIGURES

LIST OF TABLES

I. INTRODUCTION

A. BACKGROUND

In recent years Pulse Detonation Engines (PDE's) have been investigated for practical application to devices such as tactical missiles and launch vehicles. Numerous groups have begun aggressive programs to develop pulse detonation devices, among them Adroit Systems Inc., Pratt and Whitney, and Boeing. In addition to corporate initiatives there are several academic institutions that have begun active research programs. Although gas-fueled PDE concepts have been demonstrated in the lab, if the PDE is to be utilized in a tactical missile it will require the use of a liquid fuel to increase the specific energy density and reduce volume requirements.

The practice of using the energy release from a detonation is not new. Explosions have been used for over four hundred years in applications ranging from mining to fireworks. Gaseous detonations were first discovered by Bertolet at Vielle in 1881. This discovery was followed by Chapman (1899) and Jouget (1905) who independently concluded that the burnt gases propagate at sonic speed with respect to their wave front. Zeldovich, Von Neumann, and Doring independently modeled detonation waves, in the early part of the twentieth century, as shock waves followed by combustion.

The first application of a pulsed engine was the German Luftwaffes infamous "Buzz Bombs" of WWII. After the war, the United States funded a project known as "Project Squid" whose purpose was to prove the adaptability of pulse jets to both military and commercial applications. After several years of effort, all attempts were abandoned. Pulse jets utilize a deflagration process and are therefore limited by the slower flame

speeds. Pulse jets are limited to a natural operating frequency based on the geometric design of the combustion chamber. Pulse Detonation Engines (PDE's) utilize a detonation process characterized by supersonic wave speeds, in which combustion chamber pressures and frequencies are a direct factor of the geometry of the detonation environment, fuel characteristics, and valving system. The increased rate of energy conversion, higher final state pressure, and increased cycle frequency limits make the PDE concept more attractive than the pulse jet.

B. PULSE DETONATION ENGINE PRINCIPLES OF OPERATION

Many PDE's under development operate on the principal of using an ignition source to ignite a pre-mixed fuel/oxidizer mixture in a pre-detonator combustor. The mixture in the pre-detonator combustor is typically an easily detonable (fuel/O_2) mixture and will, in a short distance, transition into a fully developed detonation. This detonation wave then propagates into the main combustor, which could contain a fuel/air mixture that is not readily detonable. The energy of the entering detonation wave coupled with the geometry of the transition from the pre-detonation tube to the main combustor will eventually drive the fuel/air mixture to detonation. The main tube detonation is then initiated by the strong shock wave from the pre-detonation tube.

The purpose for using a fuel/air mixture in the main tube is explained by looking at one of the intended applications for a PDE. PDE's are being investigated as a primary source of propulsion in tactical missiles or for use in a combined-cycle with a ramjet or gas turbine engine. The use of air, as the oxidizer, in the combustor eliminates the requirement to provide additional tankage for an oxidizer. The elimination of this

requirement increases the specific impulse and allows for greater flexibility in the airframe design of the missile.

The general PDE combustion cycle, [Ref. 1], is as follows; a mixture of O_2/fuel is injected into the pre-detonation combustor at nearly the same time a fuel/air mixture is injected into the main combustor. The pre-detonation combustor is ignited and the developed detonation transitions into the main combustor, detonating the loaded fuel/air mixture. After the detonation wave exits the main combustor and the pressure bleeds down, a purge cycle is executed in which the products of combustion are blown out of the engine. The cycle is then repeated.

The frequency at which this process occurs is limited by the physical size of the detonation tube, limitations of the valving, flow rates of reactants, control program response times or by the speed at which reactants can be ignited. As the frequency of this process increases, the pressure that is realized on the head wall of the tube will approach a quasi-steady value. The time-wise, integrated pressure on the head wall will generate thrust. Thrust may also be developed from the addition of an exhaust nozzle, which would further accelerate the exiting products.

PDE's can be operated at variable frequencies, with the limitations already discussed. The inherent design of a PDE involves very few moving parts. The valving that controls the rate at which combustible materials are injected into the chambers are the only electro-mechanical parts used. The igniter is composed of solid state electronics. This reduction of critical components increases the reliability of the engine, providing a distinct advantage over normal turbo-machinery. Numerous factors affect detonations;

such as geometry of the tube, equivalence ratio, ignition energy and power level, ignition timing and aerosol size (when detonating a two-phase mixture).

A mixture of JP10 ($C_{10}H_{16}$) and O_2 was selected for this investigation. JP10 was selected primarily because of its well-known composition and for its current application in military weapons. JP10 is presently used in the Harpoon missile and has already been approved for shipboard use. A liquid fuel typically has a higher specific energy density than gaseous fuels, but utilizing a liquid aerosol significantly increases the difficulty in generating successful detonations in very short lengths. This makes the atomization and mixing of the fuel/oxidizer critical to successful detonations of liquid aerosol sprays.

II. DETONATION BACKGROUND

A. INTRODUCTION

A relevant study of a PDE must include an elementary discussion of detonations and the mechanics of detonation waves. Detonation waves are strong shock waves sustained by heat release from the combustion of highly compressed combustible reactants immediately behind the shock. The close coupling of the shock to the heat release is what defines a detonation wave.

B. DEFINITION OF A DETONATION

1. Detonation vs. Explosion

A distinction must be made between an explosion and a detonation. A thermal explosion occurs when a chemical system undergoes an exothermic reaction, whereas sufficient heat is not removed from the system and it becomes self-heating. Since the rate of reaction, and thus the rate of heat release, will both increase exponentially with temperature, the reaction rapidly runs away until the vessel containing the pressure fails; that is, the system explodes. [Ref. 2] Thus, the explosion is generally a reaction occurring within a relatively large volume. Detonations release approximately the same amount of energy as an explosion, but at a much faster rate and within a very narrow flame front.

2. Detonation vs. Deflagration

Detonations and deflagrations are both forms of combustion waves. Detonations move supersonically and deflagrations subsonically into the unburned reactants. Everyday examples of a deflagration are a campfire and a candle flame. These flames are largely governed by classical mass and thermal diffusion rates. The transport of thermal

energy and reactants is what governs the rate of flame front propagation. Detonation waves can be modeled as planar waves with reasonable results. However, the flow structure behind the shock wave is three-dimensional and strongly influences the initiation and propagation of the detonation. The detonating combustion wave speed is governed primarily by the rate of energy released by the reactants behind the shock wave. Ignition of those reactants is initiated by the thermal energy added to the reactants due to the shock compression heating.

C. MECHANICS OF DETONATIONS

1. Ignition of a Detonation Wave

There are two primary methods of initiation of a detonation wave; deflagration to detonation transition (DDT) and direct initiation. In the first, and slower method, a detonation wave velocity is reached through a transition from deflagration, which is typically ignited using a spark or flame. This method of initiation is often called thermal, or self-ignition. Thermal ignition is heavily dependent upon tube geometry (specifically length), confinement, reaction rates of the combustible mixture, and the ignition source. Thermal ignition (e.g., a spark, etc.) is most often utilized in the pre-detonator tube of a PDE.

The second method, direct ignition, is a much faster means to initiate detonation by using an ignition blast wave, or strong shock wave (e.g., a pre-detonation chamber or combustor shock wave is used to directly initiate detonation in the main combustor or main engine). Direct ignition can be accomplished by using a very high-energy spark or plasma, delivered in a very short period of time. Although this can be achieved for

certain fuel/oxygen mixtures, direct ignition of a fuel/air mixture is much more difficult to obtain.

The combustor analyzed in this paper was of the thermal ignition type and will be used as the primary ignition source for the main combustor in a PDE under development.

2. Detonation Wave Kinematics

The DDT mechanism qualitatively behaves as follows. The burned gas products from the initial deflagration wave have a specific volume on the order of 5-15 times that of the unburned gases ahead of the flame. This creates weak pressure disturbances that propagate in both directions from the combustion zone. Each succeeding compression wave tends to compress and heat the unburned gas mixture somewhat, the sound velocity increases, and the succeeding waves catch up to the initial wave. The preheating also increases the flame speed by increasing the reaction rates, which are strongly coupled to temperature. This in turn accelerates the unburned gas mixture even further to a point where turbulence is developed in the unburned gases, and compression waves are obtained. The compression waves eventually coalesce and form a shock that is strong enough to ignite the reactants. The reaction zone behind the shock sends forth a continuous compression wave that keeps the shock front from decaying and the detonation wave is obtained. [Ref. 2]

D. DEFLAGRATION TO DETONATION LENGTH

The length for the combustion wave to transition from subsonic to supersonic is typically called the deflagration-to-detonation transition length, (DDT). Shortening this length is of prime importance for both this investigation and for a tactical missile

application. The more compact that a combustor and overall engine can be made the more flexible the design can be.

1. Factors Affecting DDT Length

- DDT is highly dependent upon the combustible mixture that is being used. Some mixtures of hydrocarbon fuels and air have very long DDT lengths [Ref. 3] which may not lend themselves to practical application in a combustor. Other mixtures like, oxygen and acetylene have very short DDT lengths [Ref. 2], but are not appropriate for practical shipboard use or tactical missiles.
- Internal tube dimensions are critical for a successful transition to detonation [Ref. 2]. If the I.D. of the tube is too small a stable detonation wave cannot propagate. This will inhibit the mixture from ever transitioning to detonation. A tube that is too large will not provide enough confinement and a local source of diffractions may cause the wave to fail.
- The internal geometry of the combustor can have an effect on DDT length. By inducing a degree of wall turbulence it maybe possible to induce small vorticies along the wall of the combustor, creating small mixing zones for the fuel and oxidizer as well as creating turbulence that could aid in detonation.
- The addition of heat to the combustor can affect how quickly detonation can be achieved. Gaseous fuels and liquid fuel aerosols would be aided by being pre-heated. The heating of the liquid fuel aerosols would result in additional vaporization of the fuel on the hot tube walls and could significantly aid the combustion/detonation process.

- Equivalence ratio of the loaded "plug" of fuel has a direct effect on DDT length and whether detonation maybe achieved at all. A loaded mixture that is too lean may not provide enough fuel to the reaction zones to support a detonation; a mixture that is too rich could extract heat and inhibit a detonation wave from propagating steadily.

E. DETONATION THEORY

The calculation of detonation velocities is possible using Chapman-Jouget theory. A detailed explanation of C-J theory can be found in [Ref. 2], but it essentially assumes that detonation waves are steady, planar, and one-dimensional. With this assumption it can be shown that the flow behind the supersonic wave front is sonic relative to the wave and the point on the Hugonoit curve that represents this condition is called the upper C-J point. Looking at the wave as it moves through the tube, it is possible to determine the conditions in front of, and behind the wave, Figure [2-1].

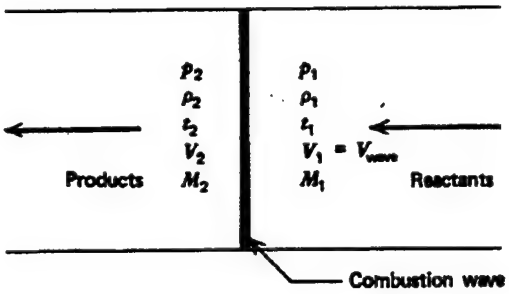

Figure [2-1]. Steady combustion wave. [Ref 4]

The Hugonoit equation can be derived from the conservation equations for the combustion wave. The derivation proceeds as follows: [Ref. 4]

$$G = \rho_1 V_1 = \rho_2 V_2 \qquad \text{(mass)} \qquad [2\text{-}1]$$

$$u_1' + p_1 v_1 + \frac{V_1^2}{2} = u_2' + p_2 v_2 + \frac{V_2^2}{2} \qquad \text{(energy)} \qquad [2\text{-}3]$$

where,

$$u' \equiv u + u^\circ \qquad [2\text{-}4]$$

In Equation [2-4] u is the sensible internal energy and u° is the internal energy of formation. Substituting Equation [2-4] into [2-3] it becomes,

$$u_1 + p_1 v_1 + \frac{V_1^2}{2} + \Delta u^\circ = u_2 + p_2 v_2 + \frac{V_2^2}{2} \qquad [2\text{-}5]$$

where,

$$\Delta u^\circ = u_1^\circ - u_2^\circ \qquad [2\text{-}6]$$

is the energy released by the chemical reaction and is called the energy of combustion. For a simple system, the caloric equation of state is given by,

$$u = u(p, \rho) \qquad [2\text{-}7]$$

Combining Equations [2-1],[2-2], and [2-5] the Hugoniot equation is obtained.

$$u_2 - (u_1 - \Delta u^\circ) = \frac{1}{2}(p_1 + p_2)(u_1 - u_2) \qquad [2\text{-}8]$$

Equation [2-7] in conjunction with Equation [2-8], specifies the allowable final states for the products behind a combustion wave for a given initial state and energy of combustion. Figure [2-2] illustrates the locus of points, plotted in the pv plane. It is known as the Hugonoit curve (H-curve) for different values of Δu°.

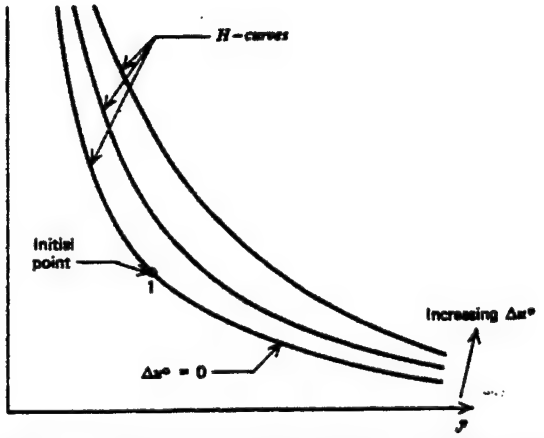

Figure [2-2] Schematic illustrations of Hugoniot curves for no reaction (Δu° =0), partial reaction (partial Δu°), and complete reaction (full Δu°). [Ref. 4]

Equations [2-1],[2-2] may be combined to yield the Rayleigh line, called an R-line. The combustion products must, therefore simultaneously satisfy the equations for the H-curve and the R-line.

When the initial and final points are plotted on the *pv* diagram (Figure [2-3]) it shows that two types of combustion processes are possible, those for which pressure and density increase are called detonation waves. Those processes for which pressure and density decrease are known as deflagration waves. This curve can further be broken down into five regions. Points J and K are the points of tangency of the H-curve with the R-Lines having the maximum and minimum slopes, respectively. They are called the Chapman-Jouget points.

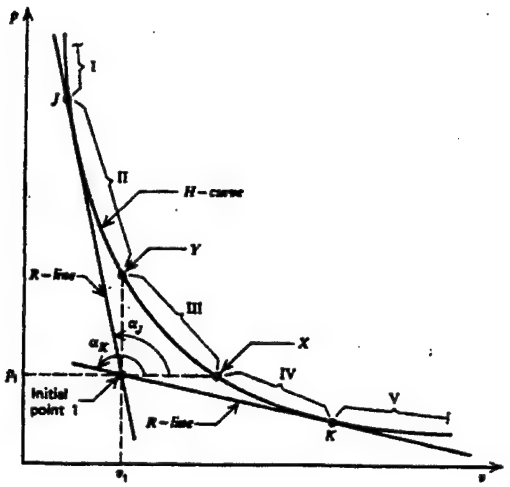

Figure [2-3]. Regions of interest on Hugoniot curve. [Ref 4]

For a mathematical treatment of the curve denote the angle between the v-axis and an R-line, α, see Figure [2-4].

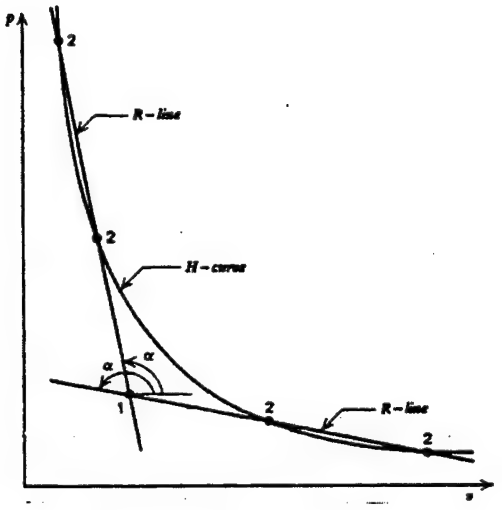

Figure [2-4]. Definition of angle α. [Ref 4]

Therefore,

$$\tan\alpha = \frac{dp}{dv} = -G^2 = -\rho^2 V^2 \qquad [2\text{-}9]$$

Hence,

$$V = \frac{\sqrt{-\tan\alpha}}{p} \qquad [2\text{-}10]$$

In the regions of the H-curve labeled I, II, IV, V, in Figure[2-5], $(\tan\alpha)$ is negative and in those regions Equation [2-10] yields physically realizable values for V. In region III, between X and Y, $(\tan\alpha)$ is positive so that V, velocity, is imaginary. Consequently, in region III, the mathematical solutions have no physical meaning, and the physically meaningful portions of the H-curve are the Regions I,II,IV,V.

Now consider point X in Figure [2-5]. Approaching the point from the physically meaningful regions of I and II, α is decreasing toward the limit of 90 deg and $(\tan\alpha)$ increasing in a negative direction toward the limit of $(\tan\alpha) \rightarrow \infty$. Consequently at point X Eqn. [2-10] yields that V behind the combustion wave is infinite.

At point Y, $\alpha = 360$ deg and $\tan\alpha$=0. From Eqn. [2-10] it is seen that the V at Y is 0. Hence the velocity of the gaseous combustion products behind the wave is zero.

Point J and K are called Chapman-Jouget points. At these points the H-curve is tangent to the R-line, Δs=0, and the velocity of the gases is exactly sonic. Figure [2-5] summarizes the types of combustion waves corresponding to the regions on the H-curve.

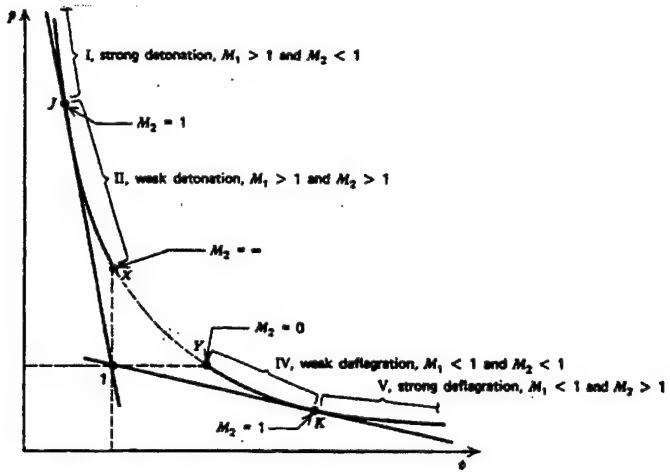

Figure [2-5]. Combustion regions on the Hugoniot curve. [Ref 4]

Region I: strong detonation, M1>1 and M2<1

Region II: weak detonation, M1>1 and M2>1

Region IV: weak deflagration, M1<1 and M2<1

Region V: strong deflagration, M1<1 and M2>1

F. ZND DETONATION WAVE STRUCTURE [Ref 1]

Zeldovich, von Neumann, and Doring (ZND) independently arrived at a theory for a simplified structure of the detonation wave. This theory states that the detonation wave consists of a planar shock moving at the detonation velocity and leaving heated and compressed gas behind it. After an induction period the chemical reaction starts and as the reaction progresses the temperature rises and the density and pressure fall until they reach the C-J values and the reaction attains equilibrium as a deflagration. A rarefaction wave, whose steepness depends on the distance traveled by the wave, then sets in to enforce the no-flow boundary conditions at the closed end of the tube. Thus behind the C-J shock, energy is generated by the thermal reaction. But, to look somewhat more

closely at the structure of the wave one must deal with the kinetics of the chemical reaction. The kinetics and mechanisms of reaction give the time and spatial separation of the shock and the heat release zone. The distribution of pressure, temperature, and density behind the shock depends upon the fraction of the material reacted. The pressure, density, and temperature profiles are very flat for a distance (induction period) behind the shock front. Then they change sharply as the reaction goes to completion at a high rate. As the gas passes from the shock front through the reaction zone its pressure drops about a factor of two, the temperature rises about a factor of two and the density drops by about a factor of three. The variations of the physical parameters can be seen in Figure [2-6]

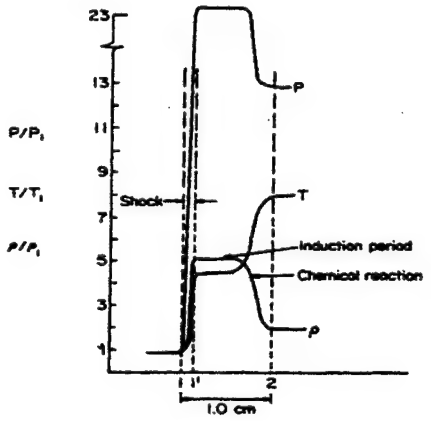

Figure [2-6]. ZND wave structure. [Ref 2]

G. CALCULATING WAVE VELOCITY

A chemical equilibrium code, PEP94, and the algorithm found in [Ref 4] were used to produce theoretical velocities of the detonation waves. The procedure to calculate the velocity is as follows:

Input the initial conditions, T_1, p_1, R_1, and C_{v1} and the mass of the reactants into

the PEP94 code. PEP is run at an estimated T_2 and p_2 to obtain values for M_2 and C_{p2}. The resulting molar species breakdown was used to compute Δu° from the standard heat of formation tables. C_{v2} and γ_2 were obtained from M_2 and C_{p2}.

Solve for T_2 by using equation,

$$T_2 = \frac{2\gamma_2}{\gamma_2 + 1}\left[\frac{C_{v1}}{C_{v2}}T_1 + \frac{\Delta u^\circ}{C_{v2}}\right] \qquad [2\text{-}11]$$

Then the density ratio can be calculated by,

$$\frac{\rho_2}{\rho_1} = \frac{\gamma_2 + 1}{\gamma_2} \qquad [2\text{-}12]$$

Then the detonation velocity can be calculated from,

$$V_w = -V_1 = \frac{\rho_2}{\rho_1}\sqrt{\gamma_2 R_2 T_2} \qquad [2\text{-}13]$$

The last step of the procedure was to calculate the pressure ratio to evaluate the initial assumption for T_2.

$$\frac{p_1}{p_2} = \frac{\rho_2 R_2 T_2}{\rho_1 R_1 T_1} \qquad [2\text{-}14]$$

The algorithm was continued until T_2 concurred with the assumed value of T_2 within +/- 5K.

The algorithm was run for several equivelance ratios. The results of these calculations are presented below in Figure [2-7].

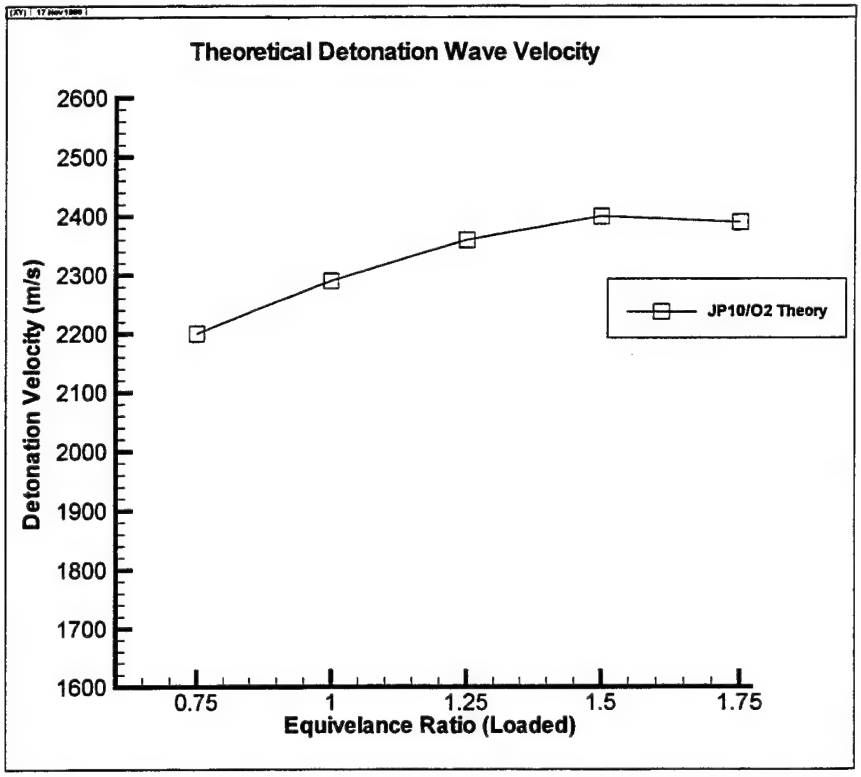

Figure [2-7]. Theoretical wave velocity.

III. EXPERIMENTAL EQUIPMENT AND CALIBRATIONS

A. PHYSICAL DESCRIPTION OF BETE NOZZLES

A search of commercially available atomizers was conducted to find one that would provide suitable droplet size, fast response times, and discrete on and off operation. The atomizer selected was the BETE XA-PR 200F with the FC2 fluid cap and the AC1503 air cap. The three inputs into the atomizer were, cylinder activation air, atomization oxygen, and pressurized fuel.

The atomization oxygen provided the internal blast-mixing of the O_2 with the fuel in the atomizer. The fuel shut-off cylinder was opened by activation air and used spring pressure to close when the supply of activation air was stopped. The on and off pulsing of the shut-off cylinder was controlled by a Peter Paul 22 Watt 24 VDC coil three-way solenoid valve and resulted in the pulsing of the fuel into the atomizer. Fuel was delivered to the atomizer at constant pressure.

Gaseous oxygen was fed directly into the atomization chamber where it mixed with the fuel. The atomization O_2 was cycled on and off using a Peter Paul 22-Watt direct acting solenoid valve. The solenoid coils were slightly overdriven with 28 volts in order to decrease valve response time. The 28 VDC solenoid power was switched by Crydom 6231 optically isolated relays with 100 microsecond response times.

B. PARTICLE SIZE DISTRIBUTION

Small droplet diameters were believed to be critical for the successful detonation of JP10 in a gaseous oxidizer environment. An approach similar to Tulis [Ref 6] was taken to model droplet heating, evaporation, and oxidation. It was concluded from the

analysis that droplets of approximately 10 microns in diameter and smaller could be heated and vaporized in the necessary time scales required for a stable detonation wave to occur.

The particle distribution and Sauter Mean Diameters (SMD) were measured using a Malvern Mastersizer particle sizing system. The measuring system was fitted with a 100 mm focal length lens, which provided approximately an 18 mm diameter measurement volume. This setup allowed particle diameter measurements from .5 to 148 microns. The nozzle was placed 5.08 cm away from the sampling volume to obtain an appropriate sample with an allowable obscuration. The experiment set-up can be seen in Figure [3-1].

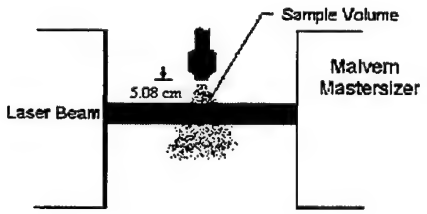

Figure [3-1]. Illustration of particle sizing experiment. [Ref. 3]

The nozzle was pulsed at numerous fuel and oxidizer pressure combinations to determine in what operating regime the nozzle would provide the smallest droplet size, while still allowing the appropriate flowrates to cover the desired O/F range. The results of these tests showed that the highest concentration by volume of small particles was obtained when the fuel pressure was operated between 40 and 50 psi and O2 was maintained between 80 and 100 psi. Results are shown in Figure [3-2], where a bi-modal particle size distribution is evident. The first mode was centered at approximately three

microns and the second at 10-12 microns. Overall, spray SMD values of below 10 μ were recorded for the wide range of fuel flows.

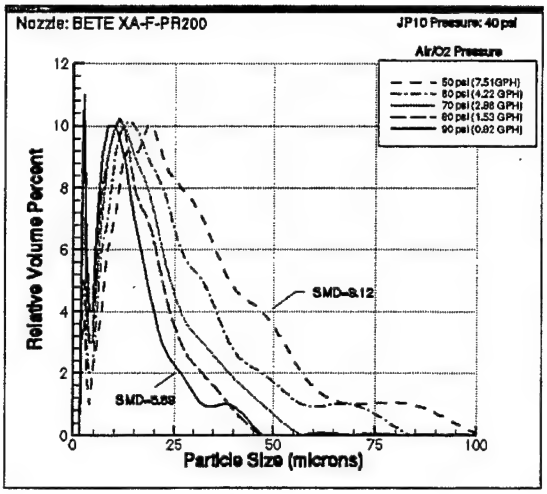

Figure [3-2]. Results of particle sizing experiments. [Ref. 3]

C. FLOW VISUALIZATION

Flow visualization was conducted by spraying the atomizer into a clear Plexiglas cylinder with the same diameter as the actual combustor. A Lexel argon-ion laser sheet was passed through the Plexiglas cylinder 5.08 cm down from the tip of the atomizer, (Figure [3-3]). The purpose of these tests was to determine qualitatively the degree of fuel impingement to the walls of the tube and the spatial uniformity of the fuel within the tube.

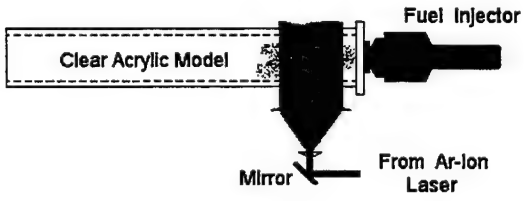

Figure [3-3]. Illustration of flow visualization setup. [Ref 3.]

The qualitative results of these tests, for the constant cross section combustor, showed an expected recirculatory pattern near the head-end, which resultsed in not only increased head-end mixing, but also in higher head-end fuel levels and a rapid pooling of fuel.

The stepped geometry (discussed below) prevented the large recirculation zone and greatly reduced fuel content on the walls.

D. NOZZLE MASS FLOW RATES AND EQUIVALENCE RATIOS

1. BETE Nozzle Flow Behavior

In order to determine the exact time at which flow into the combustor began after the activation of the solenoids, the experimental setup seen in Figure [3-4] was used. The atomizer pulse cycle, (flow on time, for both fuel and oxidizer) was varied from 10-20 milliseconds (2ms increments) and 30, 40 and 50 milliseconds. Three test sets were run at fuel and atomization pressures of 80, 92.5, 100 psig. All tests were run at three Hertz. The atomizer was exhausted into an evacuated cyclinder. The pressure rise with each injection was measured using an Omega 0-30 psia pressure transducer and recorded using a Keithley Metrabyte das 1800 data acquisistion system.

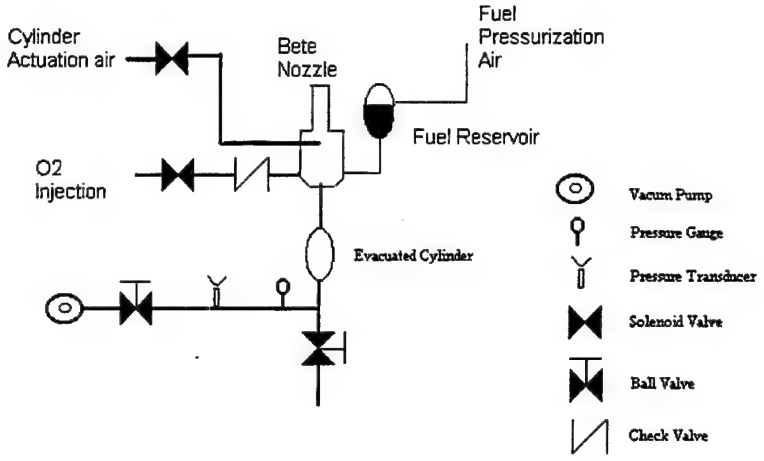

Figure [3-4]. Flow rate and valve response time experimental setup.

As seen in the results, presented in Figure [3-5], there was no appreciable flow until the flow on-time was set to approximately 14ms. This was found to be true for all pressures at which the atomizers were tested. This characteristic response time of the solenoid valves was taken into account when conducting calculations for mass flow rates and equivalence ratios.

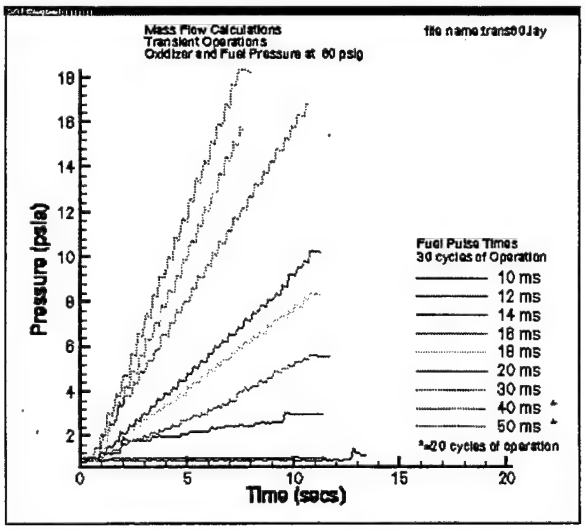

Figure [3-5]. Representative flow results for transient flow.

An overall linear increase in pressure was observed with each pulse of the nozzle for flow on-times $\geq$ 14ms. The linear trace indicates that a reasonably repeatable amount of oxygen was being injected into the combustor with each cycle.

2. Oxygen Flow Rates

The gas flow rates were determined by monitoring pressure transducers upstream and downstream of the solenoid valve, see Figure [3-6]. By recording the inlet and outlet pressures, for each cycle, it was possible to determine the flowrate of O_2 into the combustor using the characteristic flow charts and empirical calibration of the solenoid valves via the evacuated cylinder. In order to deliver the required pressure to the atomizer, a higher service pressure needed to be supplied to the upstream side of the solenoid valve due to the pressure drop across the valve orifice. The service pressure would then drop to the "inlet flow pressure" while the pressure downstream of the solenoid valve rose to the desired atomization pressure. Table [3-1] presents the required pressure settings to achieve the desired solenoid outlet pressure to the atomizer and the mass flow rate for O_2.

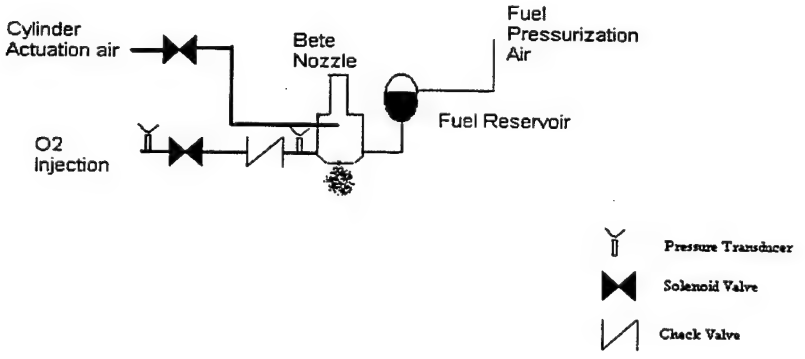

Figure [3-6]. O_2 flow measurement experimental set-up.

Service Pressure (psig)	Inlet Flow Pressure (psig)	Atomization Pressure (psig)	Flow Rate (scfm)
100	96	80	9
105	99	85	10
110	102	90	11

Table [3-1]. Pressure settings for desired O_2 pressure.

3. **Mass Flow Rates for Fuel**

Accurate measurement of the fuel mass flow for the atomizer was obtained by utilizing a 154 ml reservoir filled with water. Atomization O_2 pressure downstream of the solenoid was set at 80 psig. Cylinder actuation air was set at 80 psig. See Figure [3-7]. Fuel pressure was varied in five psig increments from 40 to 60 psig. The nozzle was then pulsed for 50 cycles over 12.5 second (4hz).

The actual flow time was 11.8 seconds. This was calculated by multiplying 14ms(solenoid time delay) by 50 (number of cycles), and subtracting it from 12.5 seconds. The amount of water discharged over this period was then measured. Mass flow rate was then calculated by dividing volumetric discharge by time and multiplying by specific density. The mass flow rate for JP10 was then obtained.

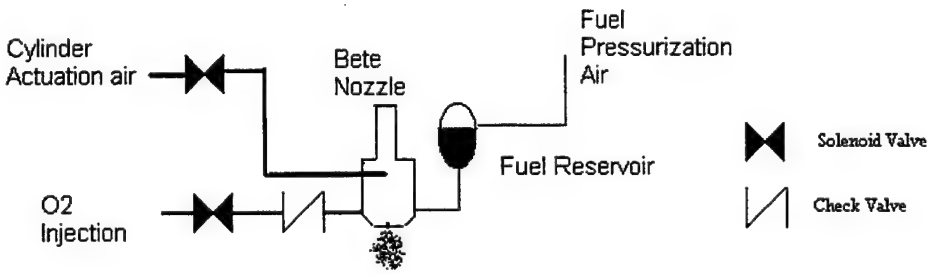

Figure [3-7]. Experimental set-up for steady-state mass flow.

The results of the mass flow measurements are presented in Table [3-2]. These results were plotted and are shown in Figure [3-8]. Mass flow rate in this operating regime was almost linear. The equation of the line allows for calculation of mass flow rate of fuel for any fuel pressure.

Atomization Air Pressure (psig)	Fuel Pressure (psig)	Volume of Water Flow (mls)	Mass Flow Rate of JP10 (gms/sec)	Mass Flow (JP10) (gms/cycle)
80	40	7	.628	.148
80	45	20	1.71	.404
80	50	34	2.88	.722
80	55	48	4.06	1.02

Table [3-2]. Fuel flow measurement results.

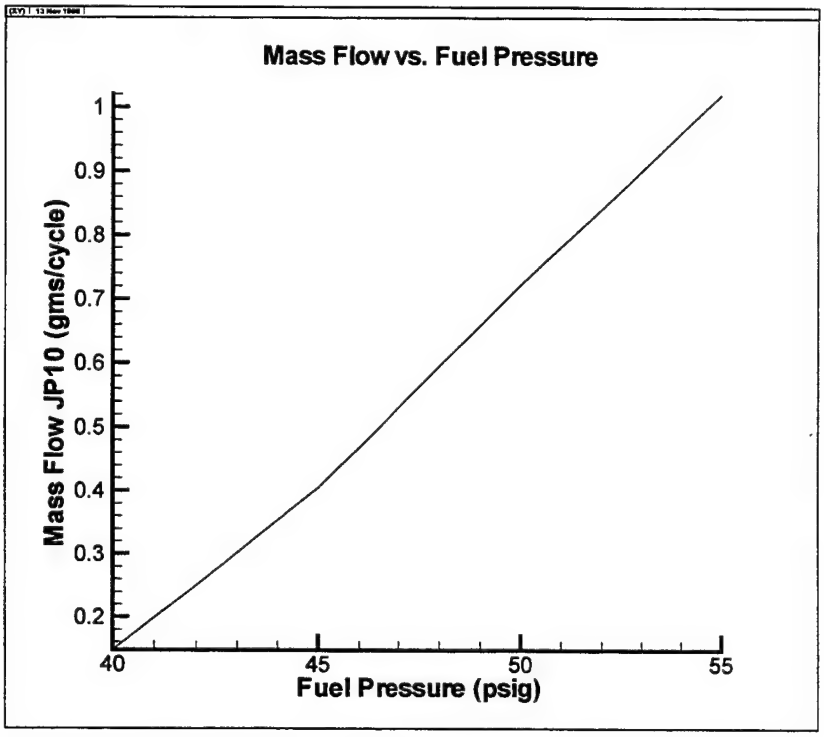

Figure [3-8]. Mass flow of JP10 as a function of fuel pressure

4. Equivalence Ratios

The stoichiometric mixture ratio for JP10 ($C_{10}H_{16}$) and O_2 is found by balancing the chemical equation for the reaction.

$$C_{10}H_{16} + O_2 \rightarrow CO_2 + H_2O$$

When balanced,

$$C_{10}H_{16}+14O_2=10CO_2+8H_2O$$

The molecular weights of the components are:

$C_{10}H_{16}$	136.24	gms
O_2	32	gms
CO_2	44.01	gms
H_2O	18	gms

The stoichiometric mixture (fuel-oxidizer) ratio for this chemical reaction is,

$$f_{st} = \frac{136.24}{448.00} = .304$$

The equivalence ratio, Φ, is obtained by dividing the actual fuel/oxidizer mixture ratio by the stoichiometric value. The actual fuel /oxidizer mixture ratio, for purposes of this paper, is defined as the mixture ratio that is leaving the atomizer or "loaded" into the combustor. The exact mixture of the fuel/oxidizer that was loaded into the combustor for each cycle was not always repeatable due to the possibility of pooling of unused fuel from previous detonations, and/or the failure of a previous detonation.

a. ***Calculation of Equivalence Ratios***

Knowing the mass flow rates for O_2 and the equation that characterized the JP10 mass flow rates made it possible to quickly calculate the equivalence ratios for all fuel and atomization oxygen pressure combinations. A Matlab program, Appendix A, was written to do all mass conversions, calculate equivalence ratios, and plot the results (Appendix B). For detailed interpretation of the plot all data points are provided in

Appendix C. The same program was used for the calculation of an O_2 flow rate of 10.5 SCFM which was necessary for the swirling O_2 experiments, see Appendices D and E.

For all subsequent testing, equivalence ratio was varied by varying fuel pressure only. O_2 pressure was constant for all tests.

E. HARDWARE DESIGN

1. Combustor

The combustor had a 3.97 cm internal diameter and was made of schedule 80 pipe. Two different lengths of pipe, 30.48 cm and 45.72 cm, were used. The head-end adapter was constructed to allow the insertion of a variable head-end geometry and to allow the swirl injection of O_2. The combustor head-end adapter is shown in Figure [3-9].

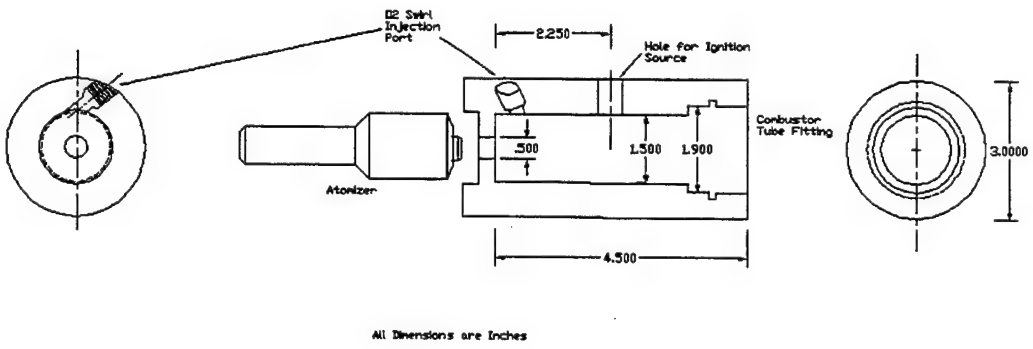

Figure [3-9]. Combustor head-end adapter.

The atomizer was bolted to the left side of the adapter while the combustor was slid into the right side and sealed with an O-ring. This design allowed the length of the

pre-detonator combustor to be varied. The tubes were tapped approximately every 2.54 cm, starting at 15.24 cm, to allow for numerous pressure measurements.

The O_2 swirl injection port was capped and the internal geometry of the adapter was not varied for the initial testing. The internal geometry was modified for one condition by sliding the divergent stepped insert, Figure [3-10], into the adapter and securing it with four 10-24 screws, producing Figure [3-11].

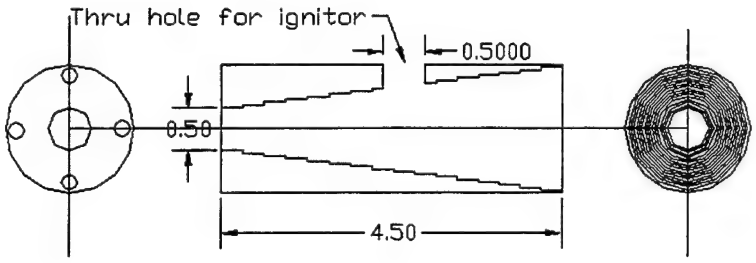

Figure [3-10]. Divergent stepped geometry insert.

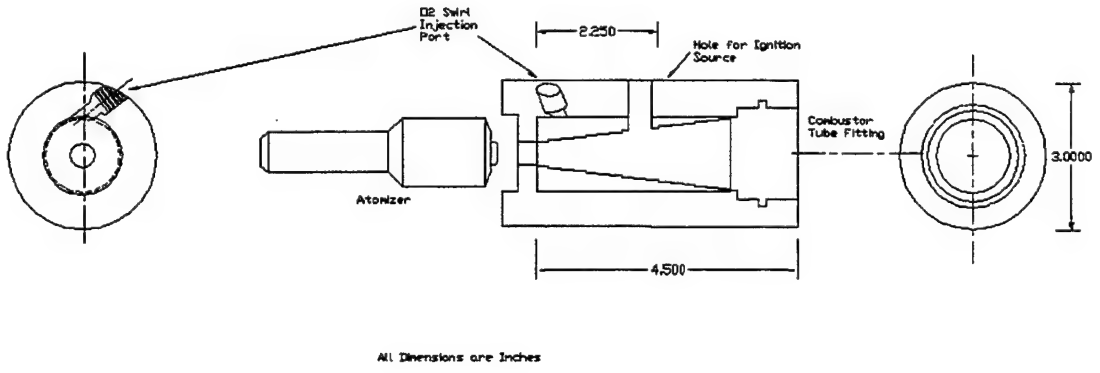

Figure [3-11]. Head-end adapter with stepped geometry inserted.

For the analysis using the O_2 swirl injection port, the stepped geometry was removed. The O_2 swirl injection flow was also provided by the same solenoid valve which provided the atomization O_2. To maintain the same atomization characteristics, a

higher upstream service pressure was supplied to the solenoid. This resulted in an over all flow rate of 10.5 scfm O_2 being injected into the combustor. Fuel flow rates were adjusted to maintain the same overall loaded equivalence ratio as in other configuration tests.

Kistler 603B1 pressure transducers and 5010B dual mode charge amplifiers with 540 kHz notch filters were used to monitor the pressure traces along the tube. The signals from the amplifiers were recorded using two Microstar Labs 3400a/415 12-bit data acquisition boards. The boards sampled at a rate of 800 kHz per channel and were synchronized to record all eight channels simultaneously in order to facilitate calculation of wave speed. Sampling at 800 kHz allowed for the collection of 1.92 seconds of data before the storage capacity on the data acquisition boards was full.

F. SOFTWARE

A Visual Basic 5.0 GUI was written to control all facility valve and ignition timing. Switching of all valving and ignition TTL signals was handled by a Keithley PIO24 board connected to a bank of Crydom 6321 solid-state relays. The solenoids used were the same solenoids that were used for the mass flowrate experiments.

The GUI made it possible to vary the frequency of detonations from 1 to 10 Hz. In varying the frequency, the total cycle time is directly affected. A complete detonation cycle consisted of injecting a fresh load of fuel and oxidizer, detonating the mixture, purging the combustion products with O_2 and then injecting a fresh detonable mixture into the chamber.

In addition to cycle time, four other timing signals could be directly controlled from the GUI. The variables were fill delay, fuel on duration, O_2 on duration and ignition delay. A brief explanation of each follows:

- Fill Delay- allows a delay from the beginning of the cycle to the time that fuel/oxygen will be injected into the detonator.
- Fuel on Duration- Time of flow for the fuel. The 14ms response lag was taken into account when this parameter was calculated.
- O_2 on Duration- Time of flow for the Oxygen. Time in excess of the fuel time is the length of time for purge. O_2 and fuel are timed to stop flowing simultaneously.
- Ignition Delay- Delay from the termination of flow of the fuel/oxidizer to the time that igniter is sparked.

The interaction of the timing parameters is displayed in Figure [3-12].

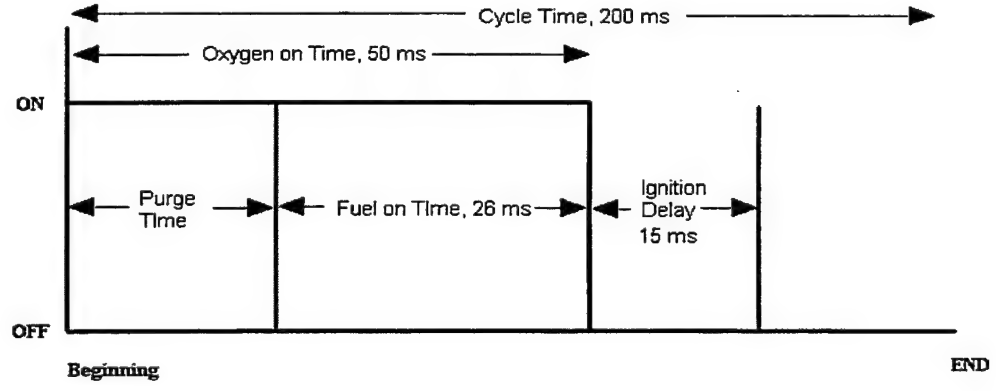

Figure [3-12]. PDE timing cycle.

G. IGNITION SOURCE

A 1.4 Joule Unison Industries ignition system was used as the ignition source for the combustor and was capable of cycle frequencies up to 10 Hz. The ignition system had an estimated delivery efficiency of 35% and was able to deliver the spark in 30-100 microseconds, resulting in power levels of approximately 4.90 kW to 16.2 kW.

H. INITIAL EXPERIMENTATION

Initial testing was conducted using the 45.72 cm long combustor to ensure adequate length for DDT. For this testing the O_2 on duration and cycle times were fixed. Fuel on duration, and ignition delays were varied until repeatable detonations occurred. Once the optimum conditions were determined the variables were fixed for the duration of the testing. Values for these variables are presented in Table [3-3]. Actual values account for the 14 ms delay for solenoid response.

Atomization air pressure was set at 80 psig for all experiments (except were noted) and equivalence ratio was varied by altering fuel pressure. Test conditions were varied from fuel-lean to fuel-rich.

Control Parameter	Value	Actual Values
Frequency	5 Hz	5 Hz
Cycle Time	200 milliseconds	200 milliseconds
Fill Delay	0 seconds	0 seconds
O_2 on duration	50 milliseconds	36 milliseconds
Fuel on duration	26 milliseconds	12 milliseconds
Ignition Delay	15 milliseconds	15 milliseconds

Table [3-3]. Timing parameters for test conditions.

IV. EXPERIMENTAL RESULTS

A. DATA ANALYSIS TECHNIQUES

1. Detonation Determination

Determination of detonation was based on three things:

- Minimum wave pressure of 300 psig

  -This requirement was based on numerous traces of non-detonation waveforms which exhibited peak pressures of up to 250 psig and propagated at velocities approaching 1000 m/s. They appeared to be a rapid deflagration event; which did not transition into a detonation over the length of the combustor. Additional detailed testing is needed to further characterize these events.

- Wave velocity approaching theoretical velocity

  -Previous non-detonation events propagated at velocities approaching 1000 m/s which did not coincide with predicted velocities on the order of 2200 m/s. To quantify a propagating waveform as a detonation a velocity approaching theoretical (Fig [2-7]) was required.

- Visible sharp pressure rise at the leading edge of the waveform as predicted in the ZND model.

  - The ZND model is composed of a normal shock coupled to a reaction zone. A very steep or almost step increase of a few hundred psi must be present to represent the existence of such a shock.

A figure representing a typical detonation test is shown in Figure [4-1]. Each pressure spike is one shot in the combustor and reflects a possible detonation. The slight decrease in baseline pressure is due to the heating effects on the pressure transducers as the test run progressed.

2. Wave Analysis

Each pressure spike with a minimum of 300 psig was evaluated at the microsecond level. The traces were examined for the sharp planar increase in pressure that was predicted by the ZND model. When it was determined that a possible detonation had developed, the velocity of the wave was computed by dividing the distance between the transducers by the time of travel of the pressure spike. V_{DDT} was computed as the average wave velocity for all the successful detonations for a particular run. Again, only a wave exhibiting pressure greater than 300 psig, planar waveform and velocity greater than 1600 m/s was considered a developed detonation. If there were less than three detonations for a run, that test condition was considered not effective.

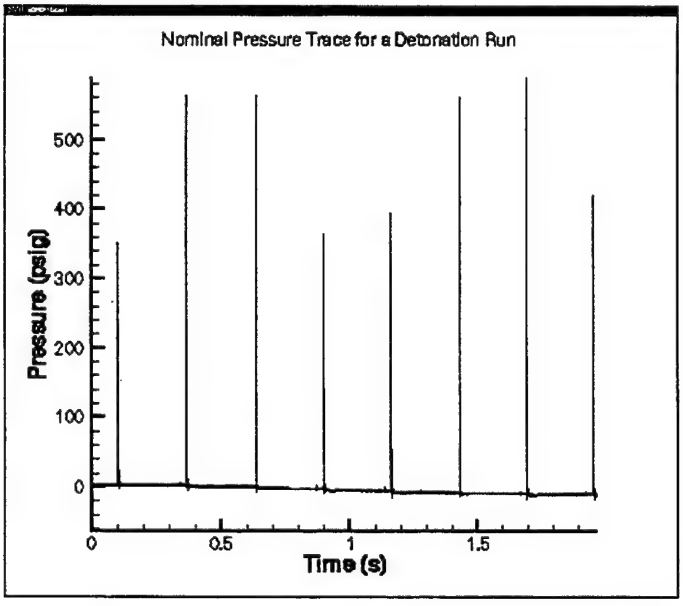

Figure [4-1]. Nominal pressure trace for a detonation run.

X_{DDT} for each test was taken to be at the transducer where the detonation wave was fully developed, see Figure [4-2]. It can be seen in the trace that the pressure wave becomes planar as it travels down the tube. At the last transducer, the wave has become planar indicating a fully developed detonation wave, (long dashed line, 35.56 cm). The distance of that transducer from the head-end was considered X_{DDT}. $\bar{X}_{DDT}$ was the average distance of all successful detonations for that run. Percent success was the ratio of successful detonations to all traces taken.

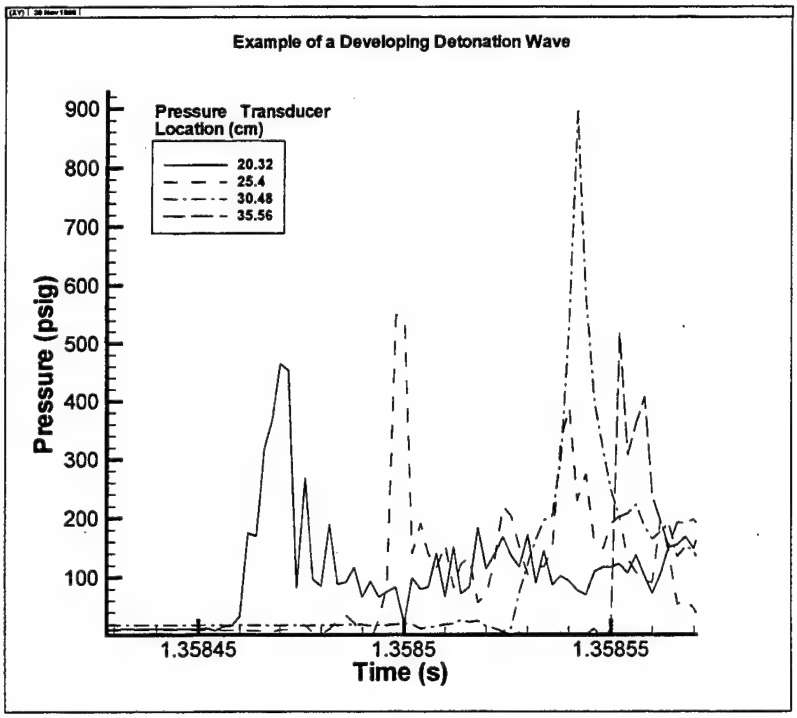

Figure [4-2]. Example of a developing detonation wave.

B. OBSERVED PHENOMENA

1. Secondary Combustion Wave

On occasion, a secondary combustion wave (Figure [4-3]) was heard following the primary combustion wave. Almost every pressure trace of the two-wave phenomena

revealed non-detonation waveforms separated by a few milliseconds. This phenomenon was observed when the combustor was cold and testing had just begun for the day. The bi-modal aerosol distribution possibly produced this effect by generating a large group of 3 μm and 10 μm droplets. It was believed that the 3 μm droplets initially were the consumed fuel source for the "first" combustion wave, which heated and vaporized the 10 μm group. After a few milliseconds, the second combustion wave then propagated down the tube.

This phenomenon was not observed once the tube temperature had increased past a temperature of 150 °F.

In Figure [4-3], the secondary combustion phenomena can be seen occurring approximately 40 ms after the initial wave. Notice that the second wave is always stronger than the first.

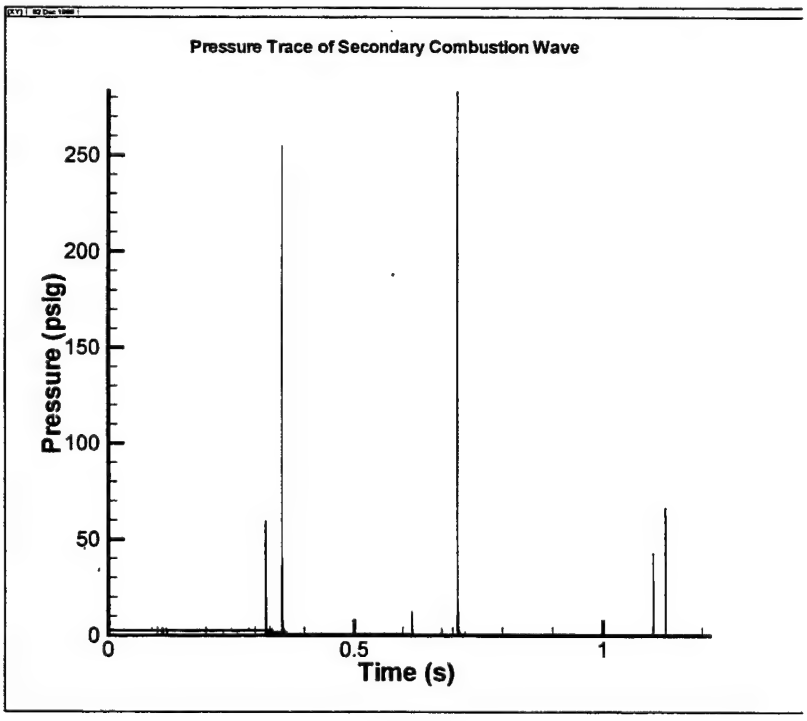

Figure [4-3]. Secondary combustion wave phenomena.

2. Explosions within Explosions

Explosions within explosions are a documented phenoma in the turbulent reaction zone, behind the incident shock. They produce secondary strong shock waves propagating in opposite directions and lateral oscillations between them. These lateral oscillations are referred to as transverse waves. The forward shock is referred to as superdetonation or "overdriven", and moves into unburned gases, and gradually decays. In the opposite direction, a shock moves into the burned gases and is known as retonation. [Ref 7].

In Figure [4-4], a situation believed to be similar to the explosion within an explosion phenomenon is visible. Additional explosions can be seen occurring at the 20.32 cm transducer, approximately 40 μs after the primary wave has passed. This is characteristic of the retonation wave. Additional retonation waves can be seen occurring at the 25.4 cm transducer. The reformed detonation wave is seen at the 30.48 cm transducer resembling a fully developed detonation wave.

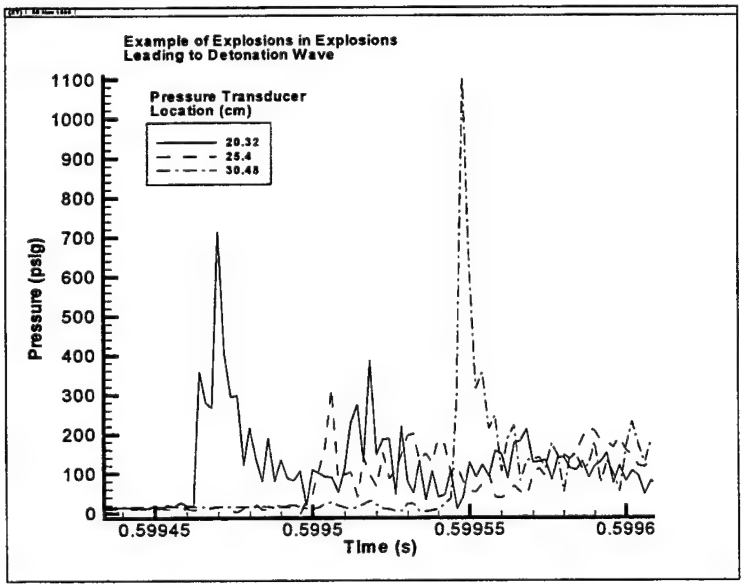

Figure [4-4]. Explosions in Explosions leading to a developed detonation wave.

C. TEST PLAN

Testing began with the constant cross-section head-end geometry and the 45.72cm length detonation tube. This was done to establish the length at which DDT would take place. Once the maximum length of DDT was established the shorter tube was used to determine the effects of heat walls, stepped divergent section, and the swirl of O_2. The results of these tests are presented in Table [4-1]. The long tube was 45.72 cm in length and the short tube was 30.48 cm in length. Ambient conditions were wall temperatures between 100-110 degs F and hot conditions were between 300-330 degs F. Temperature was measured on the outer surface of the tube.

D. EXPERIMENTAL RESULTS

Test Configuration	Equivalence Ratio	X_{DDT} (cm)	V_{wave} (m/sec)	Comparison w/Theoretical Velocity (percent)	Percent Success
Long Tube, Ambient Temp					
	.485	25.4	2221		50
	.8031	33.02	2162	99	75
	1.23	25.4	1812	78	75
	1.58	37.6	2438.	101	62.5
	2.0	38.6	2708.		62.5
Short Tube, Ambient Temp					
	No Successful Detonations				
Short Tube, Hot Temp					
	1.07	22.9	2120	92	37.5
	1.32	26.7	2540	108	37.5
Stepped Geometry, Ambient Temp					
	1.14	20.32	2088	90	37.5

Table [4-1]. Experimental Results.

Test Configuration	Equivalence Ratio	X_{DDT} (cm)	V_{wave} (m/sec)	Comparison w/Theoretical Velocity (percent)	Percent Success
Stepped Geometry, Hot Temp					
	.49	20.32	1919		37.5
	.78	19.58	1966	89	100
	1.02	20.6	2316	101	50
	1.13	20.32	2540	109	50
O_2 Swirl injection, Ambient Temp					
	No Successful Detonations				
O Swirl injection, Hot Conditions					
	1.07	22.86	2120	92	37.5
	1.32	26.7	2540	107	37.5

Table [4-1]. Experimental Results. (cont'd)

The short tube at either ambient or hot conditions did not produce detonations with an acceptable percent success. Although, it did produce a lot of rapid deflagration waveforms propagating at velocities approaching 1600 m/s.

The stepped geometry demonstrated a level of high success under hot conditions at or near an equivalence ratio of one. Velocities compared well with theoretical and overall DDT was excellent.

Another set of tests was conducted to determine if the success of the short-tube with the stepped geometry could be repeated. The results of these tests are presented in Table [4-2]. These results show that for the same test conditions the modification of one parameter can have a drastic impact on the performance of the combustor.

Test Configuration	Equivalence Ratio	X_{DDT} (inches)	V_{wave} (m/sec)	Comparison W/Theoretical Velocity	Percent Success
Ambient					
	.94	13.33	2254.33	98	37.5
Hot					
	.72	10.5	2540	113	50
	1.04	12	2398	103	75
	1.10	10	2540	110	75

Table [4-2]. Second test matrix results.

For the hot condition overall detonation was achieved at a greater length but with higher repeatability and with velocities significantly higher than those reported in Table [4-1] for similar equivalence ratios. The higher velocities observed during the second test condition may have resulted because of more fuel being consumed immediately behind the stronger shock wave.

E. ADDITIONAL TESTING

To demonstrate the flexibility of one of the PDE combustors a test case was run using the stepped geometry in the long tube, under hot conditions, but at an equivalence ratio that had not produced any successful detonations. The equivalence ratio that was used was 1.6. The fixed parameters presented in Table [3-3] were changed to reflect those shown in Table [4-3].

Control Parmeter	**Value**	**Actual Value**
Frequency	5 Hz	5 Hz
Cycle Time	200 milliseconds	200 milliseconds
Fill Delay	0 seconds	0 seconds
O_2 on Duration	50 milliseconds	36 milliseconds
Fuel on Duration	25 milliseconds	11 milliseconds
Ignition Delay	22 milliseconds	22 milliseconds

Table [4-3]. Test parameters for additional testing.

1. Test Results

Test results are presented below in Table [4-4]. Two tests were conducted to ensure reproducibility.

Configuration	Equivalence Ratio	X_{DDT} (cm)	V_{wave} (m/sec)	Comparison w/Theoretical Velocity (percent)	Percent Success
Stepped geometry, Hot Condition	1.6	20.32	2540	105	100

Table [4-4]. Test results for additional test condition.

This demonstrates that a previously unsuccessful test condition could be made successful by modifying the timing parameters alone. Thereby showing the power of a "software tunable" engine.

V. CONCLUSIONS

A. CONCLUSIONS

The combustor configuration producing the most reproducible conditions was found to be a 45.72 cm tube using a stepped divergent internal geometry. The geometry was observed to run marginally well in cold condition and improve to a 100% success rate as wall temperature increased to above 200° F. The DDT distance generally remained the same, for the hot combustor case there was a significant increase in velocity. This was likely due to the fact that as shock strength increases, a larger amount of the fuel would react immediately behind the shock, thus increasing the effective Δu° available to the detonation wave.

The successful initiation of a detonation is highly dependent upon timing of the injected materials, timing of the ignition source, and temperature condition of the tube. The numerous variables involved in operating a pulse detonation engine combustor make it very difficult to exactly reproduce conditions and results, but they do demonstrate the ability to affect engine performance and operating conditions on a cycle-to-cycle basis.

B. FUTURE WORK

Future work should involve further analysis of the effects of wall and gas temperatures on DDT, for fuel aerosols, and other possible internal configurations. A study of the effects on DDT of a variable ignition source and energy waveform would prove useful.

Computational fluid dynamic analysis of the head-end of the combustor would also provide valuable details to aid in the design of a highly efficient and effective head-end.

APPENDIX A. MATLAB CODE TO COMPUTE EQUIVALENCE RATIOS FOR NUMEROUS FUEL PRESSURES

```
%%%%This is a small program to calculate Equivelance
%%%%Ratios for multiple conditions for the Bete XA pr 200
%%%%Nozzle.


%%%%  This case is for fuel pressure from 40 psi to 55 psi.
%%%%  O2 at 80 psi



%%%%     O2 calculations

%Oxygen Flow in SCFM
O2_flow=9;

%Mass of O2 in lbs-m injected with each pulse
mass_O2=O2_flow*.014*(1/60)*(.08912);




%%%%  Mass flow of fuel.  This is for 100 data points from 40 to 55 psi.

jp10_pressure=linspace(40,55,150);              %150 datapoints
mass_flow_jp10=.00068.*(jp10_pressure)-.0254;   %flow in (gpm)

  for i=1:length(mass_flow_jp10),;

      %Computes mass of JP10 for each pulse.  Using the equation derived
      %from Figure [3-8].
      mass_jp10(1,i)=mass_flow_jp10(1,i).*((1/12.5)*(.014)*7.845);

      %Computing the Equivelance Ratio.
      ratio(1,i)=(mass_jp10(1,i)./mass_O2)/.304;


end
plot(jp10_pressure,ratio);
xlabel('Fuel Pressure (psig)');
ylabel('Equvalance Ratio');
title('Equivalance Ratios of 02 at 80 psi, 9 SCFM');


%Returning the Data to datafile to be printed out.
data(:,1)=jp10_pressure';
data(:,2)=ratio';
```

APPENDIX B. EQUIVALENCE RATIOS FOR 9.0 SCFM O_2 FLOW RATE

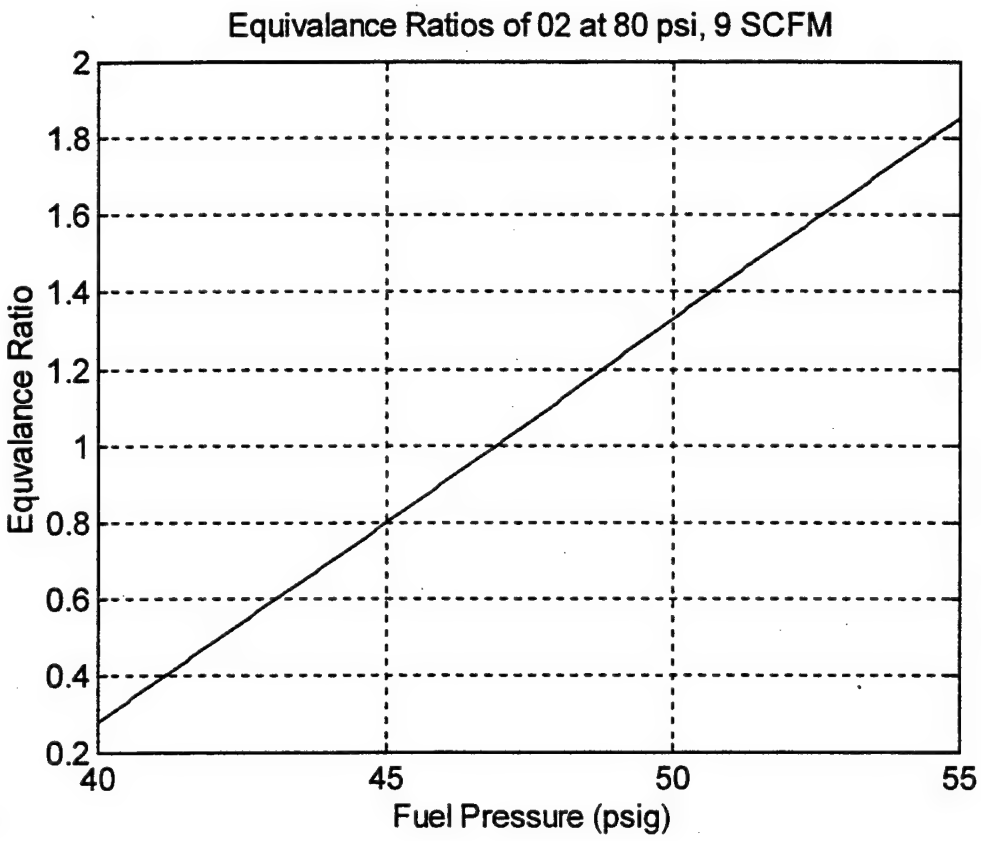

APPENDIX C. DATA POINTS USED FOR PLOT IN APPENDIX B

Data File of Equivelance ratios for 9.0 scfm flow rate of O2

Fuel Pressure (psig)	Equivelance ratio
40.0000	0.2780
40.1007	0.2886
40.2013	0.2991
40.3020	0.3097
40.4027	0.3203
40.5034	0.3308
40.6040	0.3414
40.7047	0.3520
40.8054	0.3626
40.9060	0.3731
41.0067	0.3837
41.1074	0.3943
41.2081	0.4048
41.3087	0.4154
41.4094	0.4260
41.5101	0.4366
41.6107	0.4471
41.7114	0.4577
41.8121	0.4683
41.9128	0.4788
42.0134	0.4894
42.1141	0.5000
42.2148	0.5106
42.3154	0.5211
42.4161	0.5317
42.5168	0.5423
42.6174	0.5529
42.7181	0.5634
42.8188	0.5740
42.9195	0.5846
43.0201	0.5951
43.1208	0.6057
43.2215	0.6163
43.3221	0.6269
43.4228	0.6374
43.5235	0.6480
43.6242	0.6586
43.7248	0.6691
43.8255	0.6797
43.9262	0.6903
44.0268	0.7009
44.1275	0.7114
44.2282	0.7220
44.3289	0.7326
44.4295	0.7431
44.5302	0.7537
44.6309	0.7643
44.7315	0.7749
44.8322	0.7854

44.9329	0.7960
45.0336	0.8066
45.1342	0.8172
45.2349	0.8277
45.3356	0.8383
45.4362	0.8489
45.5369	0.8594
45.6376	0.8700
45.7383	0.8806
45.8389	0.8912
45.9396	0.9017
46.0403	0.9123
46.1409	0.9229
46.2416	0.9334
46.3423	0.9440
46.4430	0.9546
46.5436	0.9652
46.6443	0.9757
46.7450	0.9863
46.8456	0.9969
46.9463	1.0074
47.0470	1.0180
47.1477	1.0286
47.2483	1.0392
47.3490	1.0497
47.4497	1.0603
47.5503	1.0709
47.6510	1.0815
47.7517	1.0920
47.8523	1.1026
47.9530	1.1132
48.0537	1.1237
48.1544	1.1343
48.2550	1.1449
48.3557	1.1555
48.4564	1.1660
48.5570	1.1766
48.6577	1.1872
48.7584	1.1977
48.8591	1.2083
48.9597	1.2189
49.0604	1.2295
49.1611	1.2400
49.2617	1.2506
49.3624	1.2612
49.4631	1.2717
49.5638	1.2823
49.6644	1.2929
49.7651	1.3035
49.8658	1.3140
49.9664	1.3246
50.0671	1.3352
50.1678	1.3458
50.2685	1.3563
50.3691	1.3669
50.4698	1.3775
50.5705	1.3880

50.6711	1.3986
50.7718	1.4092
50.8725	1.4198
50.9732	1.4303
51.0738	1.4409
51.1745	1.4515
51.2752	1.4620
51.3758	1.4726
51.4765	1.4832
51.5772	1.4938
51.6779	1.5043
51.7785	1.5149
51.8792	1.5255
51.9799	1.5360
52.0805	1.5466
52.1812	1.5572
52.2819	1.5678
52.3826	1.5783
52.4832	1.5889
52.5839	1.5995
52.6846	1.6101
52.7852	1.6206
52.8859	1.6312
52.9866	1.6418
53.0872	1.6523
53.1879	1.6629
53.2886	1.6735
53.3893	1.6841
53.4899	1.6946
53.5906	1.7052
53.6913	1.7158
53.7919	1.7263
53.8926	1.7369
53.9933	1.7475
54.0940	1.7581
54.1946	1.7686
54.2953	1.7792
54.3960	1.7898
54.4966	1.8003
54.5973	1.8109
54.6980	1.8215
54.7987	1.8321
54.8993	1.8426
55.0000	1.8532

APPENDIX D. EQUIVALENCE RATIOS FOR 10.5 SCFM O_2 FLOW RATE

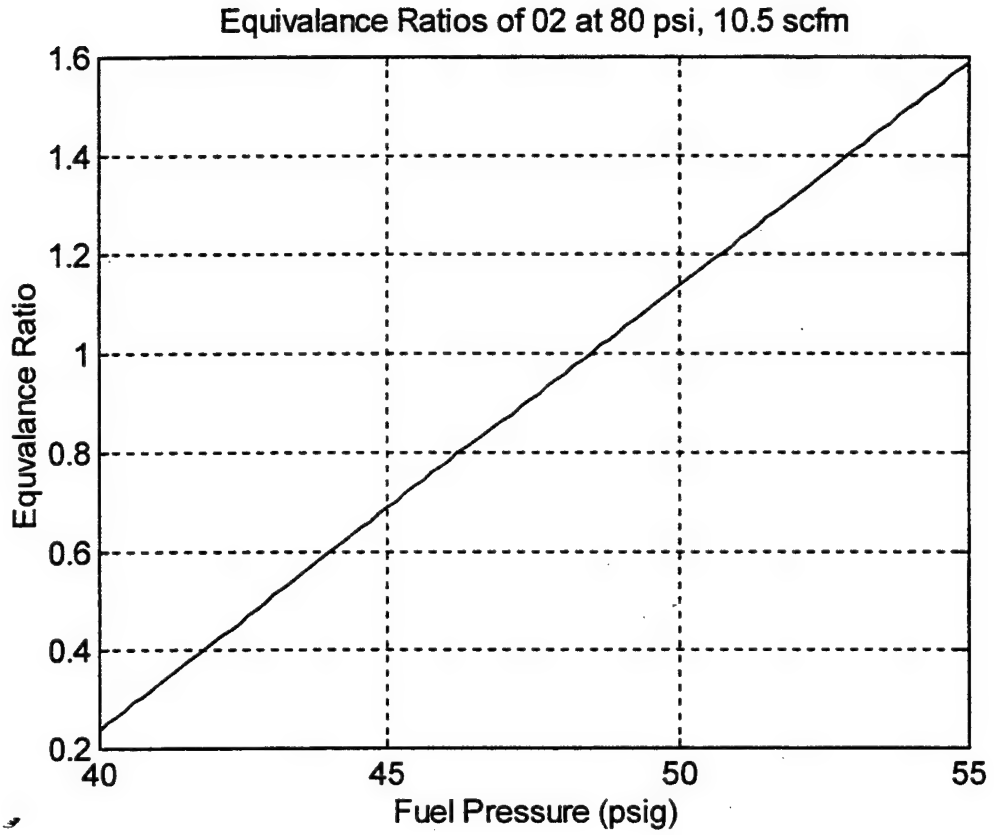

APPENDIX E. DATA POINTS USED FOR PLOT IN APPENDIX D

Data File of Equivelance ratios for 10.5 scfm flow rate of O2

Fuel Pressure (psig)	Equivelance ratio
40.0000	0.2383
40.1515	0.2519
40.3030	0.2655
40.4545	0.2792
40.6061	0.2928
40.7576	0.3065
40.9091	0.3201
41.0606	0.3337
41.2121	0.3474
41.3636	0.3610
41.5152	0.3747
41.6667	0.3883
41.8182	0.4019
41.9697	0.4156
42.1212	0.4292
42.2727	0.4428
42.4242	0.4565
42.5758	0.4701
42.7273	0.4838
42.8788	0.4974
43.0303	0.5110
43.1818	0.5247
43.3333	0.5383
43.4848	0.5520
43.6364	0.5656
43.7879	0.5792
43.9394	0.5929
44.0909	0.6065
44.2424	0.6201
44.3939	0.6338
44.5455	0.6474
44.6970	0.6611
44.8485	0.6747
45.0000	0.6883
45.1515	0.7020
45.3030	0.7156
45.4545	0.7292
45.6061	0.7429
45.7576	0.7565
45.9091	0.7702
46.0606	0.7838
46.2121	0.7974
46.3636	0.8111
46.5152	0.8247
46.6667	0.8384
46.8182	0.8520
46.9697	0.8656
47.1212	0.8793
47.2727	0.8929
47.4242	0.9065

47.5758	0.9202
47.7273	0.9338
47.8788	0.9475
48.0303	0.9611
48.1818	0.9747
48.3333	0.9884
48.4848	1.0020
48.6364	1.0157
48.7879	1.0293
48.9394	1.0429
49.0909	1.0566
49.2424	1.0702
49.3939	1.0838
49.5455	1.0975
49.6970	1.1111
49.8485	1.1248
50.0000	1.1384
50.1515	1.1520
50.3030	1.1657
50.4545	1.1793
50.6061	1.1930
50.7576	1.2066
50.9091	1.2202
51.0606	1.2339
51.2121	1.2475
51.3636	1.2611
51.5152	1.2748
51.6667	1.2884
51.8182	1.3021
51.9697	1.3157
52.1212	1.3293
52.2727	1.3430
52.4242	1.3566
52.5758	1.3703
52.7273	1.3839
52.8788	1.3975
53.0303	1.4112
53.1818	1.4248
53.3333	1.4384
53.4848	1.4521
53.6364	1.4657
53.7879	1.4794
53.9394	1.4930
54.0909	1.5066
54.2424	1.5203
54.3939	1.5339
54.5455	1.5475
54.6970	1.5612
54.8485	1.5748
55.0000	1.5885

LIST OF REFERENCES

1. Bussing, T., Pappas, G., "An Introduction to Pulse Detonation Engines", AIAA 94-0263, AIAA Inc. January 1994.

2. Glassman, Irvin, *Combustion*, Academic Press, 1986.

3. Brophy, C. M., Netzer, D.W., Forster, D.L., *Detonation Studies of JP-10 with Air and Oxygen for Pulse Detonation Development*, AIAA 98-4003, July 1998.

4. Zucrow, M. J., Hoffman, J. D., *Gas Dynamics*, John Wiley and Sons, Inc., 1977.

5. Beals, K. M., *Foundation of a Long-Term Research Effort in Liquid-Spray Detonations for Use in a Pulse Detonation Engine*, Master's Thesis, Naval Postgraduate School, Monterey, California, June 1997.

6. Tulis, A., and Selman, R., "Unconfined Aluminum Particle Two-Phase Detonation in Air", Dynamics of Shock Waves, Explosions, and Detonations Vol 94, AIAA Inc., pp. 227-292.

7. Kuo, K. K., *Principles of Combustion*, John Wiley & Sons, Inc., 1986.

INITIAL DISTRIBUTION LIST

1. Defense Technical Information Center 2
   8725 John J. Kingman Rd., STE 0944
   Ft. Belvoir, VA 22060-6218

2. Dudley Knox Library 2
   Naval Postgraduate School
   411 Dyer Rd.
   Monterey, CA 93943-5101

3. Mr. Dave Sobel 1
   Advanced Propulsion & Thermo-Fluid Systems
   United Technologies Research Center
   UTRC Mail Stop 129-29
   411 Silver Lane
   East Hartford, CT 06108

4. Dr. John Hinkey 1
   Adroit Systems Inc.
   411 108th Avenue N.E., Suite 1080
   Bellevue, WA 9800

5. CDR Roy Balaconis 1
   4349 Two Woods Road
   Virgina Beach, VA 23455-4444

6. LT Dave Forster 2
   27 Gold Street
   North Arlington, NJ 07031

7. Dr. Christopher M. Brophy, Code AA/Br 3
   Department of Aeronautics and Astronautics
   Naval Postgraduate School
   Monterey, CA 93943-5000

8. Dr. David W. Netzer, Code AA/Nt 2
   Department of Aeronautics and Astronautics
   Naval Postgraduate School
   Monterey, CA 93943-5000

9. Dr. Gabriel Roy.....1
Office of Naval Research
Mechanics Division, Office 333
Ballston Tower One
800 N. Quincy Street
Arlington, VA 22217-5660